Electronic Supplementary Material (ESI) for Biomaterials Science.

Supporting information

Advanced antifouling and antibacterial hydrogels enabled by the controlled thermo-responses of a biocompatible polymer composite

Fei Pan[a,*], Sixuan Zhang[a], Stefanie Altenried[a], Flavia Zuber[a], Qian Chen[b], Qun Ren[a,*]

a. Empa, Swiss Federal Laboratories for Materials Science and Technology, Laboratory for Biointerfaces, Lerchenfeldstrasse 5, 9014 St. Gallen, Switzerland
b. Institute of Functional Nano & Soft Materials (FUNSOM), Jiangsu Key Laboratory for Carbon-Based Functional Materials & Devices, Soochow University, 215123 Suzhou, China

*Correspondence: Fei.Pan@empa.ch; Qun.Ren@empa.ch

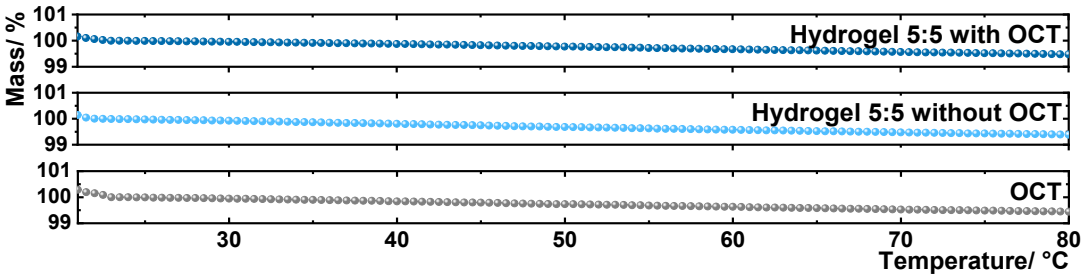

Figure S1. Thermogravimetric analysis (TGA) was applied to quantify the mass loss of a sample during the heating process to evaluate the sample's thermostability. The TGA curves of every sample displayed less than 0.7 % mass loss while heating to 80 °C, manifesting no decomposition of every sample below 80 °C and indicating an anticipated thermostability. Every sample was measured three times, and similar results were accomplished. One set of data was shown.

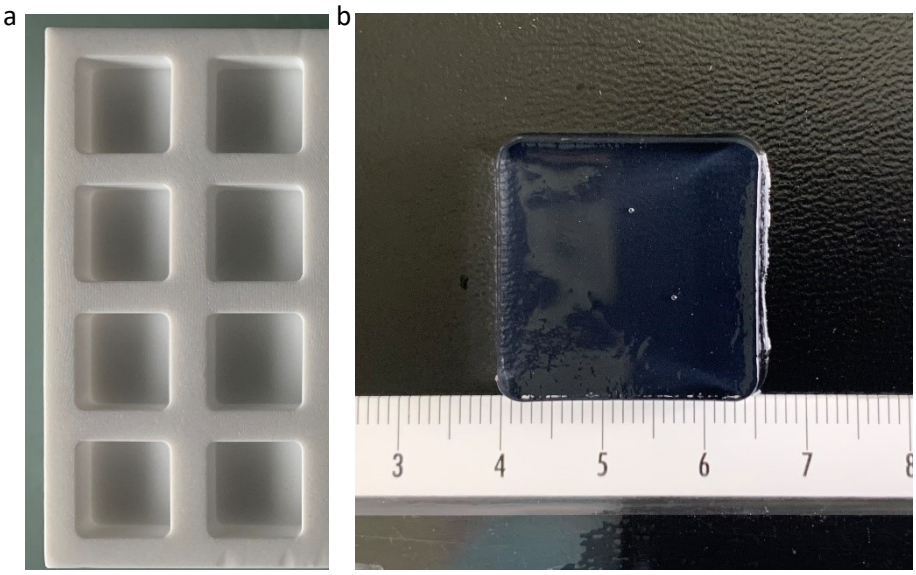

Figure S2. Hydrogel fabrication. (a) The multiwell Teflon mold (L × W × H: 1 cm × 1 cm × 0.3 cm) was used to fabricate the hydrogels before, which determined the initial size of the hydrogels before swelling. (b) Hydrogel 5:5 of the well-tuned LCST was in a well-swelling condition at room temperature.

Table S1. Analysis of thermal-regulated OCT release from OCT-loaded Hydrogel 4:6, 5:5, 6:4, and 7:3. The *in vitro* cumulative OCT released from hydrogel samples was listed for time points of 10, 30, 60, 120, 240, 360, and 600 minutes. The standard deviation was derived from three replicates of every measurement, and the release analysis was performed three times. One set of measurements was demonstrated.

Time / minute	OCT amount released from different hydrogel samples/mg ·L^{-1}							
	Hydrogel 4:6		Hydrogel 5:5		Hydrogel 6:4		Hydrogel 7:3	
	30 °C	37 °C	30 °C	37 °C	30 °C	37 °C	30 °C	37 °C
10	1.57 ± 0.22	1.68 ± 0.74	0.06 ± 0.12	2.43 ± 0.54	0.09 ± 0.15	2.07 ± 0.75	0.07 ± 0.11	2.55 ± 0.22
30	2.74 ± 0.42	2.86 ± 0.53	0.22 ± 0.09	4.12 ± 0.43	0.27 ± 0.22	3.97 ± 0.54	0.22 ± 0.13	4.23 ± 0.41
60	4.79 ± 0.41	5.05 ± 0.47	0.32 ± 0.11	6.45 ± 0.74	0.31 ± 0.18	6.68 ± 0.67	0.34 ± 0.12	6.94 ± 1.01
120	4.84 ± 0.34	5.12 ± 0.42	0.41 ± 0.13	10.77 ± 0.88	0.44 ± 0.16	9.88 ± 0.89	0.39 ± 0.17	11.26 ± 1.07
240	4.88 ± 0.22	5.17 ± 0.54	0.72 ± 0.12	13.75 ± 0.45	0.78 ± 0.10	12.97 ± 0.64	0.74 ± 0.19	15.43 ± 0.78
360	4.77 ± 0.52	5.20 ± 0.44	0.95 ± 0.25	16.84 ± 1.23	0.89 ± 0.33	17.27 ± 0.99	1.01 ± 0.33	17.44 ± 1.44
600	5.07 ± 0.44	5.24 ± 0.77	1.52 ± 0.31	21.96 ± 2.88	1.48 ± 0.42	22.03 ± 1.03	1.44 ± 0.37	22.46 ± 2.56

Table S2. The corresponding table of Table S1 displaying OCT release in percentage.

Time / minute	OCT amount released from different hydrogel samples/%							
	Hydrogel 4:6		Hydrogel 5:5		Hydrogel 6:4		Hydrogel 7:3	
	30 °C	37 °C	30 °C	37 °C	30 °C	37 °C	30 °C	37 °C
10	29.85 ± 4.18	31.94 ± 14.07	0.27 ± 0.55	11.05 ± 2.45	0.41 ± 0.68	9.34 ± 3.38	0.31 ± 0.49	11.31 ± 0.98
30	52.09 ± 7.98	54.37 ± 10.08	1.00 ± 0.41	18.73 ± 1.95	1.22 ± 0.99	17.91 ± 2.44	0.98 ± 0.58	18.76 ± 1.82
60	91.06 ± 7.79	96.01 ± 8.94	1.45 ± 0.50	29.32 ± 3.36	1.40 ± 0.81	30.13 ± 3.02	1.51 ± 0.53	30.78 ± 4.48
120	92.02 ± 6.46	97.34 ± 7.98	1.86 ± 0.59	48.95 ± 4.00	1.98 ± 0.72	44.56 ± 4.01	1.73 ± 0.75	49.93 ± 4.75
240	92.78 ± 4.18	98.29 ± 10.27	3.27 ± 0.55	62.50 ± 2.05	3.52 ± 0.45	58.50 ± 2.89	3.28 ± 0.84	68.43 ± 3.46
360	90.68 ± 9.89	98.86 ± 8.37	4.32 ± 1.14	76.55 ± 5.59	4.01 ± 1.49	77.90 ± 4.47	4.48 ± 1.46	77.34 ± 6.39
600	96.39 ± 8.37	99.62 ± 14.64	6.91 ± 1.41	99.82 ± 13.10	6.68 ± 1.89	99.37 ± 4.65	6.39 ± 1.64	99.60 ± 11.35

Table S3. Surface mechanical properties of hydrogel 5:5 without and with the loading of OCT. Young's modulus and surface adhesion force was measured by AFM-force spectroscopy. Three replicates of every hydrogel sample were characterized, and 576 indentations of every replicate were executed to derive surface Young's modulus, adhesion force, and corresponding standard deviation. Student's *t*-test ($p < 0.01$) for both hydrogel samples revealed no significant difference regarding surface Young's modulus and surface adhesion, respectively. But a significant difference in surface adhesion forces was noted between both hydrogel samples and the mPEG surface.

Sample	OCT loading	Surface Young's modulus/kPa	Surface adhesion/pN
Hydrogel 5:5	No	180.2 ± 45.4	112.2 ± 31.6
Hydrogel 5:5	Yes	179.3 ± 46.8	118.1 ± 35.2
mPEG	-	-	475.7 ± 23.5

Video legends:

Video Graphic Abstract. The designed drug release mechanism of hydrogel upon triggering the thermo-switch.

Video 1. The process animation to measure single molecular adhesion force between human serum albumin (HSA) and a material surface.

Video 2. The process animation to immobilize a normal human dermal fibroblast (nHDF) on a tipless hollow cantilever (Micropipette, Cytosurge AG, Switzerland) with a nominal spring constant of 2 $N \cdot m^{-1}$.

Video 3. The process animation to measure single cell adhesion force between an nHDF and a material surface.

Video 4. The process animation to immobilize a bacterium on a pyramidal hollow cantilever (Nanopipette, Cytosurge, Switzerland) with a nominal spring constant of 2 $N \cdot m^{-1}$ and a 300 nm aperture at their distal end.

Video 5. The process animation to measure single bacterial adhesion force between a bacterium and a material surface.